NOVEL ZINC ALLOY CASTINGS FOR MEDICAL IMPLANTS

Thomas Yuen

Bachelor of Engineering
Mechanical Engineering

Department of Mechanical Engineering
Macquarie University

November 06, 2017

Supervisor: Professor Candace Lang
Co-supervisor: Dr Wei Xu

ACKNOWLEDGMENTS

I would like to acknowledge, my parents for their support throught out my bachelor's degree. To my friends whom has helped throughout each semester. To my academic supervisors Professor Candace Lang and Dr Wei Xu for providing assistance on this thesis and to Wendy Tao, Mynga Nguyen and Chao Shen for providing assistance and supporting during the operation of the equipments.

STATEMENT OF CANDIDATE

I, Thomas, declare that this report, submitted as part of the requirement for the award of Bachelor of Engineering in the Department of Mechanical Engineering, Macquarie University, is entirely my own work unless otherwise referenced or acknowledged. This document has not been submitted for qualification or assessment an any academic institution.

Student's Name: Thomas Yuen

Student's Signature: 

Date: 6/11/2017

ABSTRACT

There have been many studies of biodegradable metals, mainly involving magnesium and iron, with new studies of zinc. Zinc being an essential element of the human body and biocompatible, this makes it a potential candidate of biodegradable metal. However zinc is brittle and have low mechanical properties, but excel in corrosion resistance. Therefore the focus of this research is to experiment with different composition of magnesium and calcium, to see how they affect the characteristics of zinc. With the success of the characterisation, it will lead onto using the zinc-alloy in 3-d printing for medical implants.

Contents

List of Figures

List of Tables

Chapter 1

Introduction

After many years of minimising the corrosion of metallic biomaterials, there has been a new interest of incorporating biodegradable metals in medical applications. The definition of biodegradable metals is that the metal is expected to degrade over time, also assisting in healing of the body part and leaving no residue. Therefore, the major factor of biodegradable metals should consist of the essential element that can metabolised in the human body. When testing the metal, it must be biocompatible of which it must not cause any adverse pathophysiological and toxicological effect. With the use of biodegradable metals this reduces the need for secondary surgery to remove the implants. When working with biodegradable metals the elements may suffer from rapid corrosion or it may not have a decent mechanical properties. To prevent these factors, different techniques are used to improve the chemical and mechanical properties, these techniques include applying a coating on the surface of the metal or introducing a new element into the metal, resulting in an alloy [2]. This project will look into forming an alloy with zinc, using magnesium, calcium and strontium.

Magnesium has attracted a great interest in biodegradable materials as it can degrade in the human body and is also non-toxic. But the disadvantage of magnesium is that it degrades to rapidly, therefore further studies are considering using a new metal, zinc.

Zinc is essential to the human body as it is important to the function of enzymes, such as the immune system. It also supports the healing of the wound and normal growth. Therefore being a great candidate for biodegradable metal [3]. The reason for choosing a metallic biodegradable material compare to polymers and ceramics is that they have a higher strength, hardness and fracture toughness.

1.1 Project Goal

The research topic of this project is 'Can a novel zinc-magnesium alloy be successfully characterised, and successfully 3-d printed?'. The first task of this project is to research what metallic elements can be used to form an alloy with zinc. The element must meet several requirements, which consist of being biodegradable, non-toxic to the human body (biocompatible), have a good mechanical property and a low melting temperature. The main objective of this project is to successfully characterised the alloy; what are the mechanical properties and microstructures of the unique alloy. The reason for this type of characterisation is important for any new material which has not been characterised and for any alloy which is proposed as a 3-d printing candidate.

Chapter 2

Literature Review

2.1 Biodegradable Metals

2.1.1 Biocompatibility of alloy

For an alloy that is used as a medical implant it must be biocompatible. For it to be biocompatible it must serve for a long period without a negative response, as it is intended to be applied in connection with living tissue. All medical applications, require the alloy to not release any toxic ions. Beside it being non-toxic, it must be capable of co-existing with the human tissue also without causing damage to the body system. When developing a new biomaterial it must be relevant to where the implant will be placed. An example would be a knee replacement will require a biomaterial, that is biocompatible, high corrosion resistance and wear resistance. Whereas for a cardiovascular stents, which doesn't stay in the body for a long period, therefore a material that will degrade quickly than the one used for knee replacement.

Table 2.1: Elements that exist in the human body

Element	Wt.%	At.%
Oxygen	65.0	25.5
Carbon	18.5	9.5
Hydrogen	9.5	63.0
Nitrogen	3.3	1.4
Calcium	1.5	0.31
Phosphorus	1.0	0.22
Potassium	0.4	0.06
Sulphur	0.3	0.05
Sodium	0.2	0.3
Chlorine	0.2	0.03
Magnesium	0.1	0.1
Trace element	<0.01	<0.01

Table 2.1 shows the elements normally found in the human body. When developing a biomedical alloy, the alloy should consist of those found in the human body or a reactive alloy, such as titanium [1].

2.1.2 Pure zinc and zinc alloys

Zinc is a metal found in the earth's crust. It is primarily used for preventing corrosion in different metals, through coating or alloying with another element. However zinc is soft, brittle and have a low mechanical strength. The mechanical properties are; tensile strength of below 20 MPa, the elongation = 0.2% and Vickers hardness = 37 [4]. Therefore, further research is required to achieve the necessary mechanical properties to be applied in medical applications.

With the ongoing research of biodegradable metals, different zinc alloys are experimented to achieve the desired mechanical properties which would benefit biomedical implants. By experimenting with different zinc alloys, they are able to determine how each element of different composition affect the properties of zinc. The elements that are chosen for forming zinc alloys, are magnesium, calcium and strontium. These elements were selected because of how they interact with the human body, such as being available in the human body and not affect or disrupt the function of the human body.

As mentioned, zinc is an essential element in the human body, as more than half of it is found in muscle tissue. Zinc is important to the function of several enzymes and it supports the immune functions and wound healing [5]. The reason why zinc is the main focus is that the corrosion rate is better for clinical application rather than iron and magnesium alloys. Not only does it have better corrosion rate, zinc based alloy has a low melting point, therefore it can be prepared easily.

Zn-Mg

According to many different articles the most investigated alloy is Zn-Mg, this being Mg is an element that had been regularly utilised in medical implants. Those sources suggest that Zn-Mg alloy containing 1-3 wt.% Mg is the best composition, which improves the tensile strength and the ductility of pure Zn [6]. However when more magnesium are introduce into the alloy it reduces the strength, plasticity and toughness, shown in figure 2.1. Therefore the ideal magnesium concentration is between 1-2 wt.%.

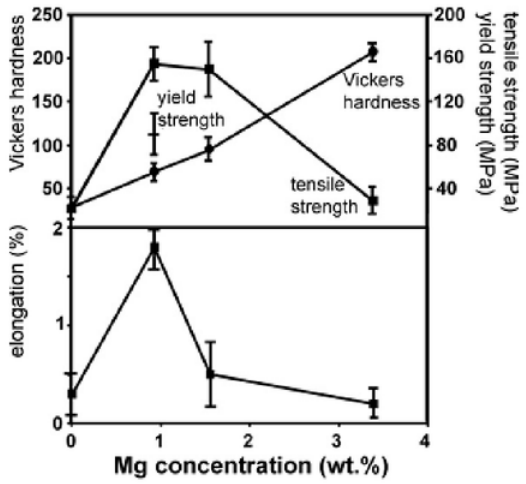

Figure 2.1: Mechanical properties of the Zn-Mg alloy versus Mg content [5]

2.1.3 Magnesium and Mg alloys

As mention in section 2.1.2, magnesium has been widely studied as a biodegradable metal. This is because magnesium exhibits excellent mechanical properties and biocompatibility [2], resulting in Mg-based implantable medical devices such as cardiovascular stents and bone fixation plates, pins and screws. Since magnesium is a biodegradable metal such as zinc, there is no need for secondary surgery to remove the implants. However the main problem of magnesium is its rapid biodegradation, this causes the mechanical integrity of magnesium to fail which also leads to a build up of hydrogen evolution, retarding the healing process [5] [6].

To prevent the rapid degradation different methods are used. These methods consist of alloying with an element or coating. However with coating there are pros and cons. The pros being it won't change the mechanical properties of magnesium, whereas the material used in coating Mg may affect the biocompatibility [2]. The other solution consists of

alloying with different elements such as RS66 a magnesium alloy with composition of Mg–6.0% Zn–1.0% Ce–0.6% Zr [7]. The studies of Willbold et al. managed to maintain the alloy's structural architecture for long period and corrode slowly [7]. This shows that it is possible to improve the mechanical properties of a element.

2.1.4 Strontium

Strontium, Ca and Mg belongs to the group 2 of the periodic table and shares similar physical and chemical properties of calcium. It is softer than calcium, with a melting point at 777°C. The average adult has an daily intake of 2 mg, this suggest that the element is biocompatible. Sr is an element that can found in the human body and mainly found in the bones [8]. Since Sr is closely related to Ca it is a good candidate for alloying with Zn and the effects on the mechanical properties and biocompatibility can be investigated.

Chapter 3

Experimental Procedures

Before going into the practical side of this project, the first step is to determine the composition of each alloy, shown in table 3.1. All materials were purchased through a supplier in the form of shots, granular and turnings, this allow for easy measurement. The next step is to calculate the ratio of atomic to weight percentage, the element is then weighted according to the calculations. The two elements are then melted in the Hot Platinum induction furnace at 27% power output with argon flowing into the crucible, reducing the oxygen around the materials and preventing it from any oxidation. The alloy is heated to a temperature around 500°C, metal becoming dark red. The alloy is left in the crucible to be cast, forming a small ingot.

3.1 Microstructures

After forming the alloy it is then cut to size (fitting the 30mm dia. mould) with the silicon carbide wheel at 1800rpm and a feed speed of 0.06mm/s, shown 3.1. Once the samples have been cut to size it is then mounted onto a mount. The material use for the mount will be polyfast, which is conductive, allowing it to be use in the SEM(3.2). Next the samples were first grinded using SiC grinding foils (Grit 320 and 1200), next polished with diamond pastes of 3, 1 and 0.04µm particles (Mol R and Nap R and OP-S) (3.3). The final step of preparing the microstructure is to etch the sample in a solution of 5% nitric acid and water; 1min 30secs for Zn-Mg and around 3 - 4mins for Zn-Ca and Zn-Sr. A more detailed method for grinding and polishing shown in figure A.1.

3.2 Microscopy

The microstructures of the alloys were examined by using an Optical and a Phenom Scanning Electron Microscope. The Phenom SEM will produce images of the surface topography through Secondary Electrons and through Backscatter Diffraction, images consist of microstructures, texture, defects and grain morphology. 10 kV is used as the recommended settings for BSD for high resolution images. Next the composition can

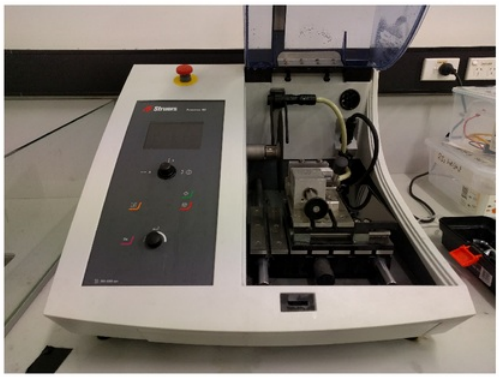

Figure 3.1: Cutting Machine from Struers

Figure 3.2: Mounting Machine from struers

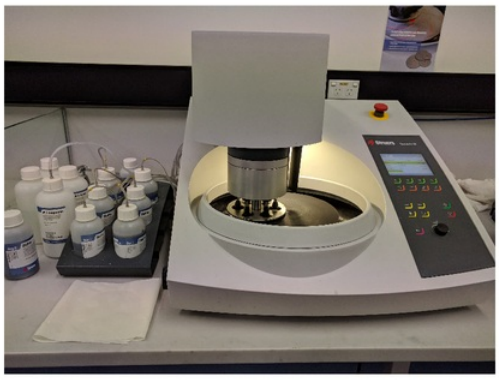

Figure 3.3: Polishing and Grinding Machine

be examined by using the SEM through Energy-dispersive X-ray spectroscopy (EDS) method with 15kV intensity, point can be selected for point analysis and map for line scan or mapping. The Optical microscope can be used to analysis the surface of the sample quickly and produces good quality image. The recommended lens for the zinc alloys is 10X.

3.3 Mechanical Properties

A Vickers Hardness Test from struers was used to measure the hardness value of the samples. Each sample were required different loads to obtain a consistent value during the analysis. The loads are as follow;

- HV2 for Zn-Mg
- HV0.3 for Zn-Ca
- HV0.05 for Zn-Sr

3.4 Calculation

at.% to wt.%
x = element 1
y = element 2

$$wt.\% = \frac{(at.\%x)(at.wt.x)}{(at.\%x)(at.wt.x) + (at.\%y)(at.wt.y)} \times 100 \tag{3.1}$$

example of Zn 99 at.%

$$wt.\% = \frac{(99)(65.38)}{(99)(65.38) + (1)(24.305)} \times 100 = 99.63\ wt.\%$$

Table 3.1: Compositions of the studied materials (in at.%)

Materials	Zn 1	Mg	Ca
Zn	99.99	-	-
Zn-1 Mg	99	1	-
Zn-2 Mg	98	2	-
Zn-3 Mg	97	3	-
Zn-4 Mg	96	4	-
Zn-5 Mg	95	5	-
Zn-1 Ca	99	-	1
Zn-2 Ca	98	-	2
Zn-3 Ca	97	-	3
Zn-4 Ca	96	-	4
Zn-5 Ca	95	-	5

Chapter 4

Results

This chapter examines the microstructures and the hardness values of each zinc alloys, allowing for comparison to see which alloy meets the requirements.

4.1 Pure Zinc

Zinc of 99.7% were used to set a base result to compare against when other elements are added to it. The important step in this thesis were to make an alloy. Testing were undertaken to see what power percentage were able to melt zinc.

Table 4.1: Testing induction furnace for sufficient power

Power	**Time**	**Results**
15%	1min	Nothing happened, zinc did not melt
20%	1min	Zinc is starting to change
27%	1min	Zinc has started melting but only 1 part not melted
27%	2min	Oxidation started to form, white substances similar to webs were forming around the zinc and crucible
23%	3min	Trying a low power setting for longer period, only resulting in a bright flash

Table 4.1 shows the power and time tested to see what the appropriate method to melt zinc and zinc alloy. The testing above were all done without argon flowing through into the crucible therefore in one of the tests, oxidation started to form. The best method tested is 27% with time of around 1-2min. In the next testing argon were available, as a result the zinc were melted without any issue. During the next testing the induction furnace ran at a power of 27% for 1 minutes 20 seconds, at the 30 second mark the zinc

started to melt, as the colour of the zinc turned a faint red around 500°C. Next was to test a larger piece of zinc at 20 grams, this took 2 minutes and 30 seconds. This confirms that the power setting at 27% is the preferred settings. Figure 4.1 shows the mounted zinc with polishing and etching.

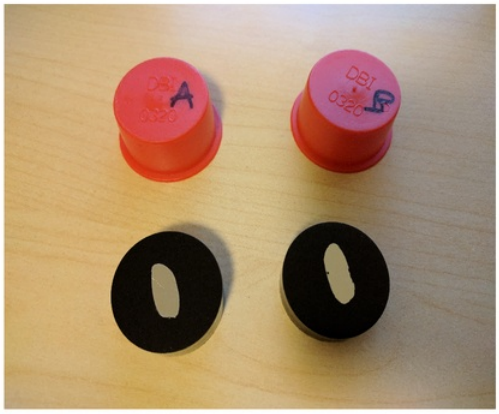

Figure 4.1: Mounted Zinc

4.1.1 Hardness Test

The average hardness value for pure Zn are 55HV. This value will be used to compare the hardness value of each alloys. The reason for zinc's low hardness value are the large grain structures.

Table 4.2: Hardness Values for Pure Zinc

HV used	HV
0.5	55.2
0.5	50.8
0.5	55.2
0.5	48.1
0.5	61.1
0.5	58.5
0.5	56.1
Average	55

4.1.2 Microstructures

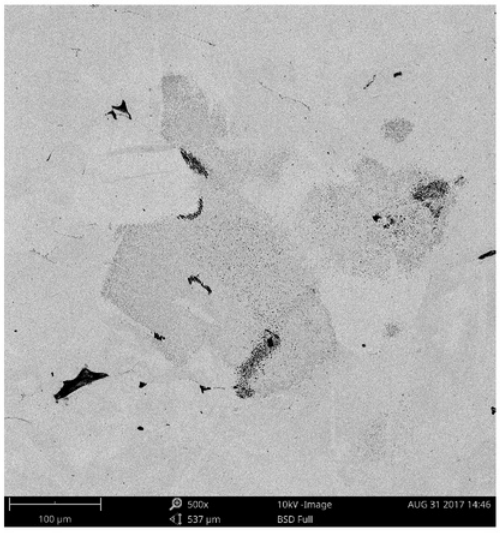

Figure 4.2: BSD image of Zn from SEM

Figure 4.2 shows the surface morphology of pure zinc, it is clear that pure zinc contains large grain structures with size greater or equal to 100 µm.

4.2 Zn-0.8Mg

The next step, were to melt zinc and magnesium to form an alloy of magnesium 1 - 5 at.%. Testing were also required to see if the induction furnace were able to melt the two elements and form an alloy before an actual run is attempted. Zinc shots at 99.99% and magnesium turning at 99.99% were used.

- 1st test with Zn-Mg the elements did not melt.
- 2nd test ran for a longer period resulted in only the elements on one side that were touching the ceramic crucible melted.
- 3rd test with 30% power was unsuccessful, still couldn't get the Zn shots to melt.
- Final test were to try with a solid rod zinc and observe if the Mg will melt into the Zn. The results were that Zn did melt but Mg didn't.

From the test the zinc shots and magnesium turnings were unable to melt due to the shots and turnings size not getting enough heat transfer. Therefore it has concluded

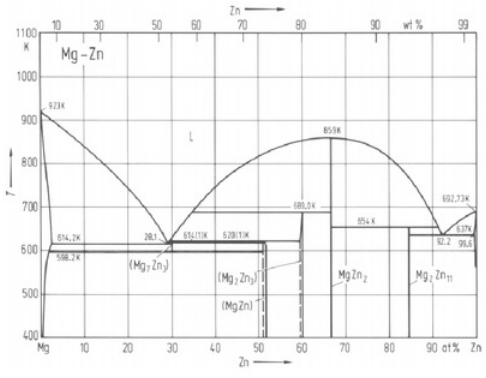

Figure 4.3: Zn-Mg Phase Diagram [9]

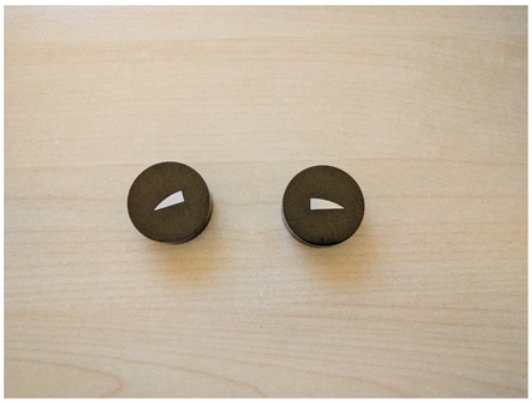

Figure 4.4: Zn-0.8Mg

that using the supplied ceramic crucible it were not able to melt, so a graphite crucible were select to overcome the heat transfer inhibition could be the solution in melting the elements. When the graphite crucible were available and testing were under way, an unfortunate event occur as there were are problem with the induction furnace thus the process of making an alloy were dismissed. A sample of as-cast zinc-0.8 wt.% magnesium was obtained through Dr Wei Xu, this thesis' co-supervisor. The samples were also heat treated to a temperature of 300°C and 200°C for 1 hour and analysed. This was done to see if there would be any change affecting the microstructures and mechanical properties.

4.2.1 Hardness Test

For the hardness test HV2 was used to measure the hardness of Zn-0.8Mg and heat treated samples. The mechanical properties of Zn-0.8Mg and the heat treated samples are summarised in table 4.3, 4.5, 4.4. It can be observe that the hardness of Zn-Mg increases with magnesium concentration. This can be accounted for the eutectic mixture with Zn and the intermetallic phase of Mg_2Zn_{11} shown in figure 4.10 being very fine. There were a slight change in hardness value when the Zn-Mg were heat treated, to further understand the change a in-depth analysis of the grain is needed to see if there were changes in size but time did not permit.

Table 4.3: Hardness Values for Zn-0.8Mg

Force	Hardness Value
HV2	76.5
HV2	79.6
HV2	73.5
HV2	75.1
HV2	78
HV2	77.7
HV2	77.5
Average	76.8

Table 4.4: Hardness Values for Zn-0.8Mg, heat treat at 300°C

Force	Hardness Value
HV2	81.6
HV2	81.3
HV2	86.7
HV2	81.1
HV2	80.4
HV2	84.1
HV2	81.1
Average	82.4

Table 4.5: Hardness Values for Zn-0.8Mg, heat treat at 200°C

Force	Hardness Value
HV2	84.2
HV2	83.2
HV2	82
HV2	84.3
HV2	90
HV2	79.8
HV2	79.4
Average	83.3

4.2.2 Microstructures

Backscatter Diffraction

Figure 4.5 and 4.6 shows the microstructures of Zn-0.8Mg. It can be observed that the alloy are hypoeutectic because they consist of large Zn crystals (lighter shade) with sizes ranging from 50 to 100µm and an eutectic mixture of Zn and Mg_2Zn_{11} (darker) which had a lamellar structure located at the grain boundaries, this is verified in figure 4.9. For the heat-treated samples according to the phase diagram, there should not be much change with the zinc crystals, whereas the eutectic mixture will become closer shown in figure 4.9. Through the SEM images it is difficult to determine whether there is change between the as-cast Zn-Mg and the heat-treated, 200° and 300°.

EDS

Figure 4.9 shows the mapping of Zn-Mg alloy, the red represents the concentration of Mg_2Zn_{11}. As observed there is an eutectic mixture between the zinc grains. In table 4.6 it shows the concentration of zinc and magnesium in figure 4.9. Magnesium weight concentration of 0.6 wt.% came relatively close to 0.8 wt.% this may be due to the mapping being concentrated in a small area, if the area of the mapping were not to zoomed in, the value of the weight percentage would be around 0.8%. Observing the Zn-Mg phase diagram (4.3) the intermetallic phase should be Mg_2Zn_{11}, the calculation below shows that the concentration of Mg at that point should 15 at.% which is relatively close to the data in table 4.7.

$$\begin{aligned} 2 &= \text{Magnesium} \\ 13 &= \text{total of Mg2 + Zn11} \\ \frac{2}{13} &= 15at.\%Mg \end{aligned}$$

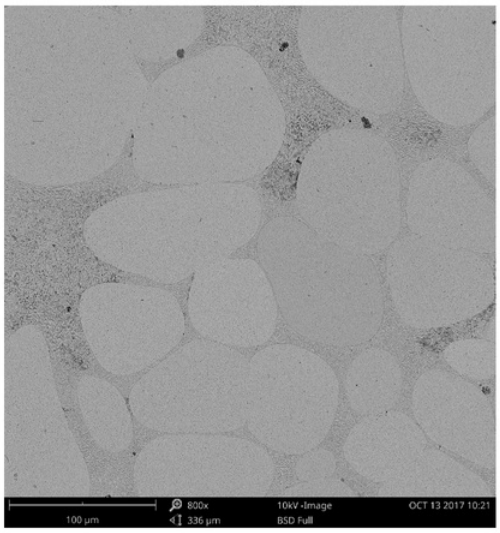

Figure 4.5: SEM of Zn-0.8Mg (800x)

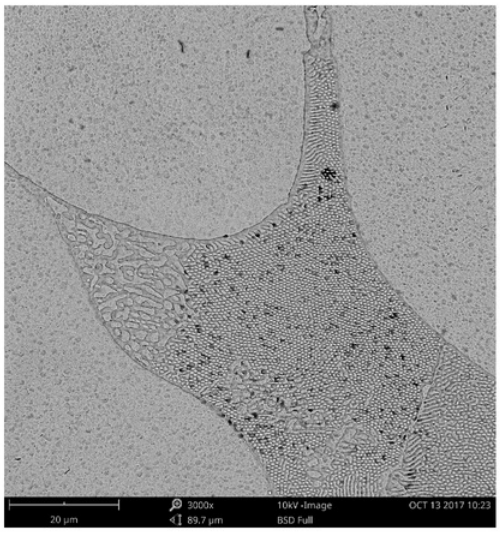

Figure 4.6: SEM of Zn-0.8Mg (3000x)

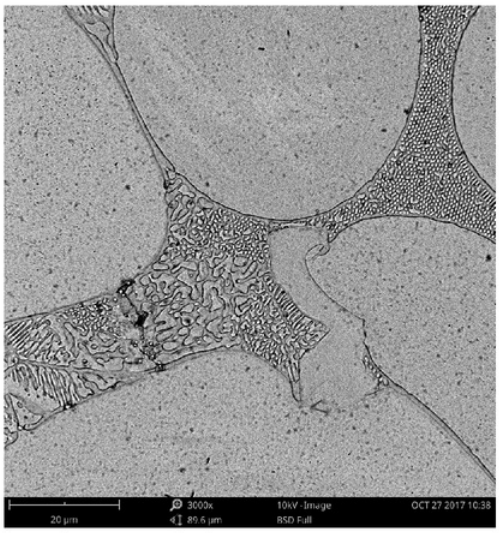

Figure 4.7: Microstructure of Zn-0.8Mg heat-treat at 200°C

Table 4.6: Mapping Data of Zn-0.8Mg (fig.4.9)

Element Number	Element Symbol	Element Name	Atomic Conc.	Weight Conc.
30	Zn	Zinc	98.40	99.4
12	Mg	Magnesium	1.60	0.60

Table 4.7: Spotting Data of Zn-0.8Mg (fig.4.10)

Element Number	Element Symbol	Element Name	Atomic Conc.	Weight Conc.
30	Zn	Zinc	88.85	95.54
12	Mg	Magnesium	11.15	4.46

Figure 4.8: Microstructure of Zn-0.8Mg heat-treat at 300°C

4.3 Zn-0.8Ca

Calcium is another element that can be alloy with Zn to form a biodegradable metal. As a result of the furnace not working, different at.% composition were not available to be compared with each other to determine which is best. The sample provided by Wei Xu, the thesis' co-supervisor is as-cast with a 0.8 weight percentage of Ca.

4.3.1 Hardness Test

The hardness test started out with the force HV2 but was not able to get a proper reading, as the indentation were deformed. The force was lowered till the reading were stable of HV0.3. The result shown is that there wasn't an increase in hardness from pure zinc shown in table 4.8, the reason for this may be due the microstructures of the alloy (4.14).

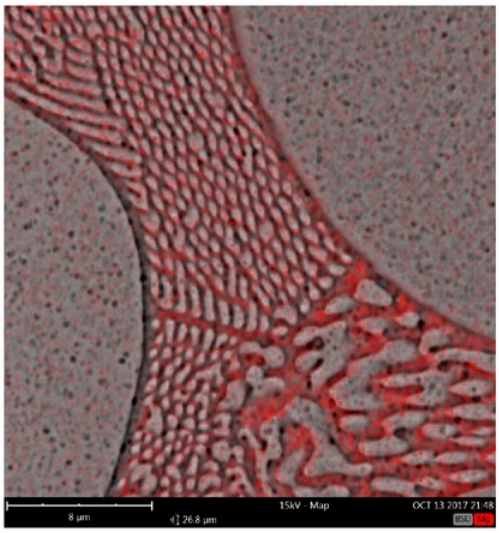

Figure 4.9: Mapping of Zn-0.8Mg

Table 4.8: Hardness Values for Zn-0.8Ca

Force	Hardness Value
HV0.3	61.6
HV0.3	53.9
HV0.3	43.9
HV0.3	48.9
HV0.3	41.7
HV0.3	55.8
HV0.3	50.7
Average	50.9

4.3.2 Microstructures

Backscatter Diffraction

Figure 4.13 shows the microstructures of Zn-0.8Ca. As observe the zinc (dark) is surrounding the intermetallic phase of the calcium (light). Compare to the Zn-Mg alloy the intermetallic phase is enriched with calcium instead of the eutectic structure which is the cause of the higher hardness value. The size of the calcium varies as some are ranging from 20µm to 100µm. The Secondary Electron Detector provides the topography of Zn-Ca alloy which gives a clearer image in identifying the different grain boundaries of the alloy but also includes the contamination on the alloy. It can be seen in figure 4.13 there

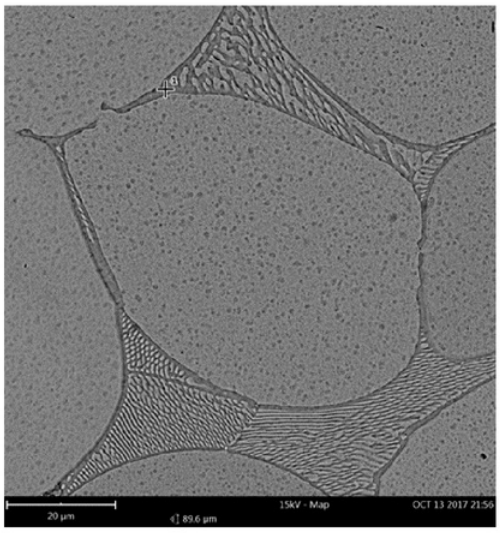

Figure 4.10: Spot of Zn-0.8Mg

are many black particles affecting the quality of the image. This is due to the alloy being contaminated from the residue after it were polish and etched. Therefore the Zn-Ca alloy were re-polished and the surface cleaned with the ultrasonic cleaner, to rid of any excess particles. The re-polished alloy weren't etched to see if the SEM provided a clearer image (figure 4.15). But in return the grain boundaries were difficult to identify and also due to using a non-conductive mount for the SEM. The image capture of Zn-0.8Ca from the optical microscope seen in figure 4.16, shows a clear image of the intermetallic phase of enriched calcium. It also shows that the calcium are different sizes.

EDS

The EDS were able to capture the present of calcium shown in figure 4.18 and managed to provide the correct wt.% concentration of calcium in the alloy. Figure 4.17 highlights in red the position where the calcium is situated. Comparing figure 4.17 to figure 4.9 it is proven that the intermetallic phase is very different as the majority of the element is calcium and not a mixture. According to the phase diagram (4.11) the intermetallic phase closest to 0.8 wt.% is $CaZn_{13}$. A point is used to determine the at.% of calcium which matches the intermetallic phase by calculating the ratio of Ca to the total ($\frac{1}{14} = 7at.\%$). Shown in table 4.10 the 5.58 at.% is relatively close to 7 at.% therefore proving that the intermetallic phase are made up of $CaZn_{13}$.

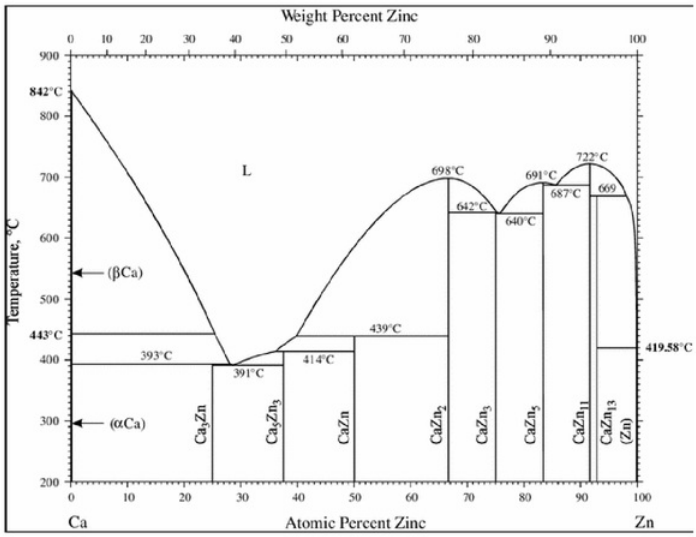

Figure 4.11: Ca-Zn Phase Diagram [10]

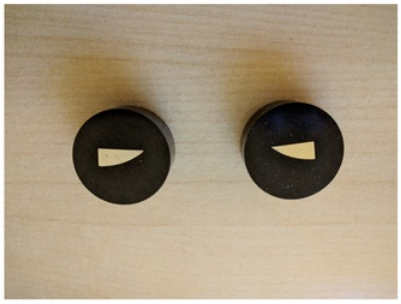

Figure 4.12: Zn-Ca

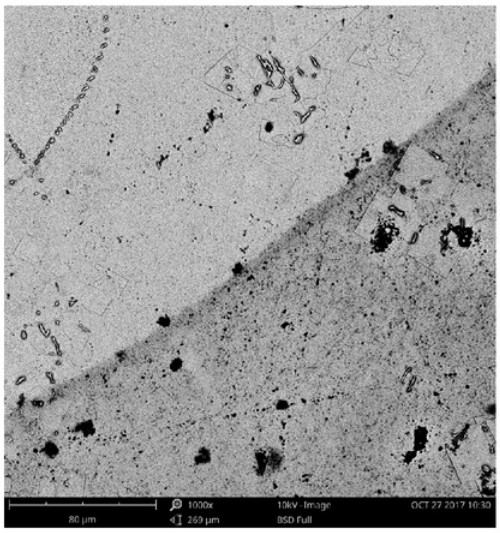

Figure 4.13: BSD image of Zn-0.8Ca

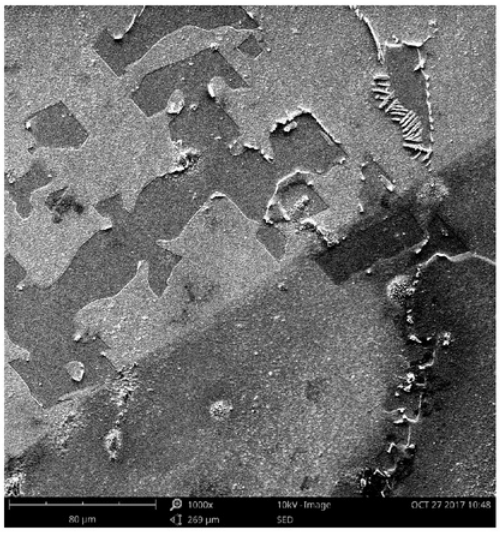

Figure 4.14: SED of Zn-0.8Ca

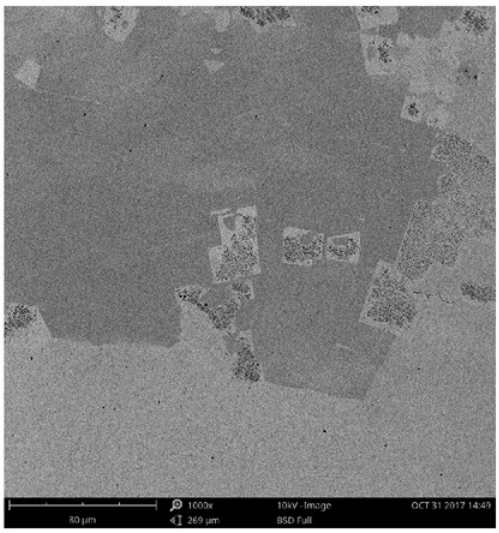

Figure 4.15: Not etched BSD image of Zn-0.8Ca

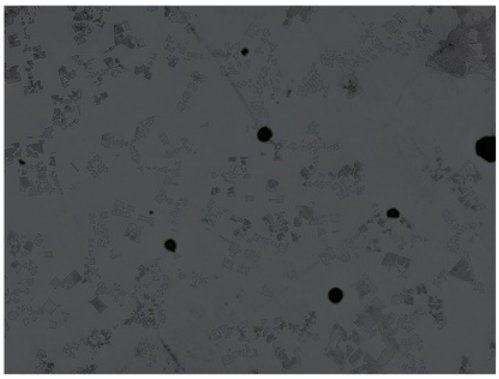

Figure 4.16: Micrograph of ZN-0.8Ca from Optical Microscope

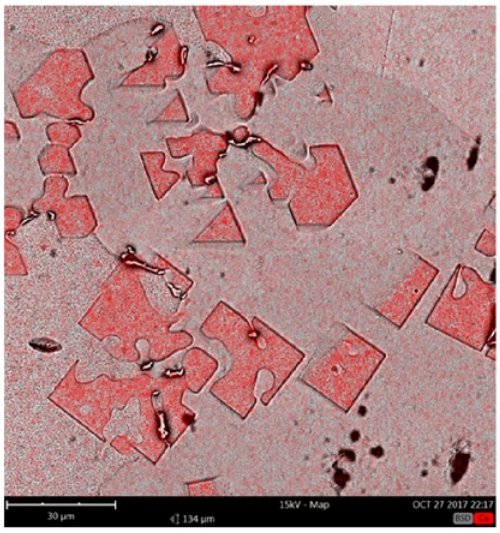

Figure 4.17: Combined mapping of Zn-0.8Ca

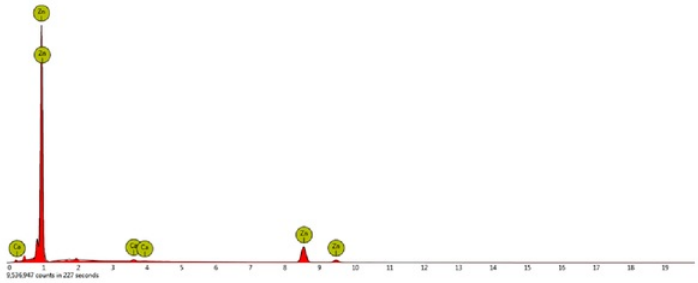

Figure 4.18: Mapping process of Zn-0.8Ca

Table 4.9: Mapping Data of Zn-0.8Ca (fig.4.18)

Element Number	Element Symbol	Element Name	Atomic Conc.	Weight Conc.
30	Zn	Zinc	98.64	99.16
20	Ca	Calcium	1.36	0.84

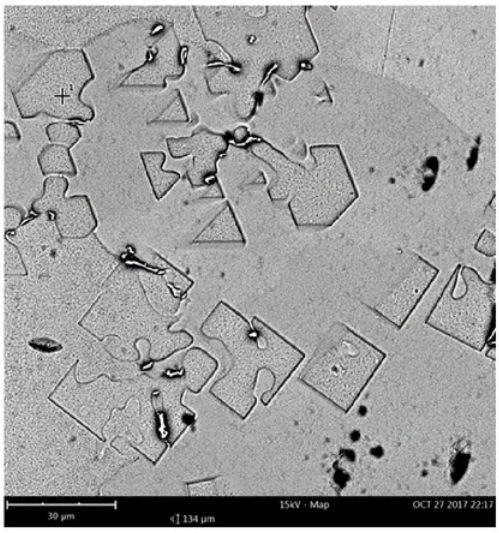

Figure 4.19: Point of Zn-0.8Ca

Table 4.10: Point Data of Zn-0.8Ca (fig.4.19)

Element Number	Element Symbol	Element Name	Atomic Conc.	Weight Conc.
30	Zn	Zinc	94.42	96.5
20	Ca	Calcium	5.58	3.5

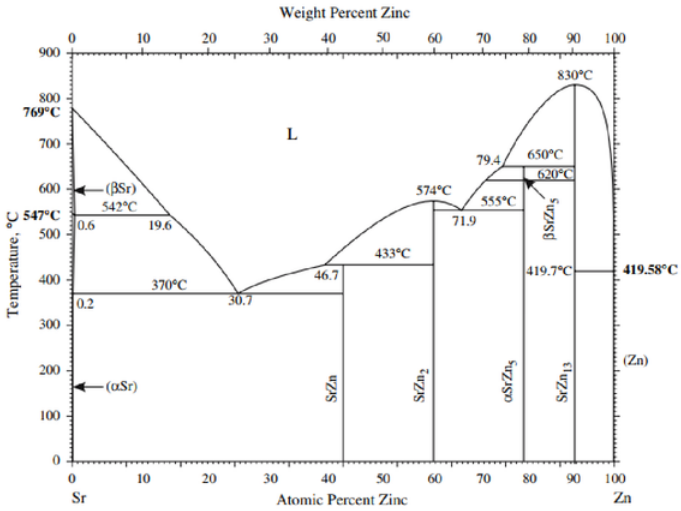

Figure 4.20: Sr-Zn phase diagram [11]

4.4 Zn-0.8Sr

This sample were also provided by Dr Wei Xu. The composition of the alloy is 0.8 wt.% strontium and it is also as-cast. This section includes the characterisation of Zn-Sr alloy.

4.4.1 Hardness Test

Same with calcium a reading was not obtained with forces HV2 and HV0.3, therefore a lower force was required (HV0.05). With much patience the hardness value of Zn-Sr alloy were obtained (table 4.11). The average hardness value of Zn-Sr is 42.9 which lower than pure zinc but according the article 'Development of biodegradable Zn-1X binary alloys with nutrient alloying elements Mg, Ca and Sr' [4], Zn-Ca should have a hardness value around 70. There may be some discrepancies from the measuring of the hardness or the making of the Zn-Sr alloy.

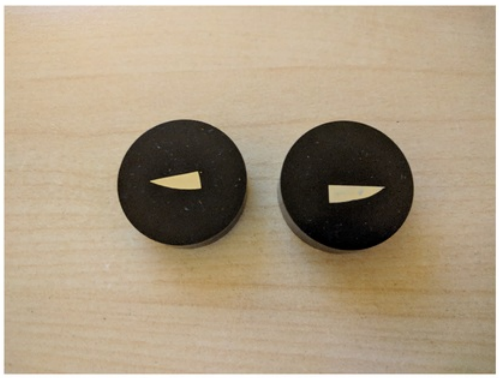

Figure 4.21: Zn-0.8Sr

Table 4.11: Hardness Values for Zn-0.8Sr

Force	Hardness Value
HV0.05	40.6
HV0.05	45
HV0.05	45.5
HV0.05	41.4
HV0.05	40.6
HV0.05	45
HV0.05	42.7
Average	42.9

4.4.2 Microstructures

Backscatter Diffraction

In figure 4.22 the lighter shade is strontium whereas the darker is zinc. The intermetallic phase of the alloy tend to be a solid shape which is enriched with Sr and smaller in size of 20µm (4.23). The strontium enriched, tend to be at a distance from one another which is the cause of the Zn-Sr alloy having a possible low hardness value in comparison to pure Zn. Figure 4.22 also consist of many small black particles which not be present. This was caused when the surface of the alloy hasn't been cleaned properly, see figure 4.24. Figure 4.25 captures the micrograph of Zn-0.8Sr from the optical microscope at 10X.

EDS

Through the EDS, the concentration of strontium is 1.41 wt.% and the sample is said to have 0.8 wt.% of Sr. The values are relatively close but a longer and high quality EDS

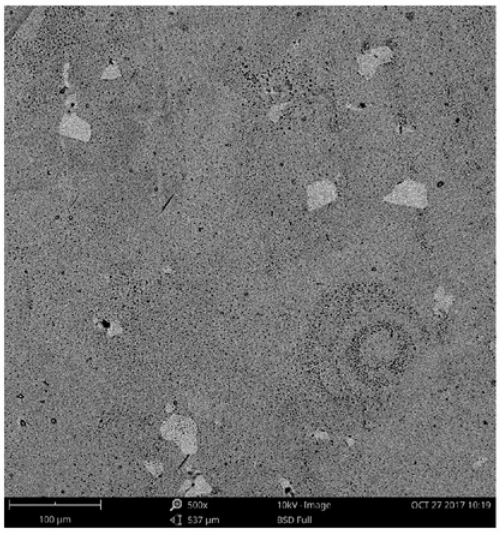

Figure 4.22: BSD image of Zn-0.8Sr

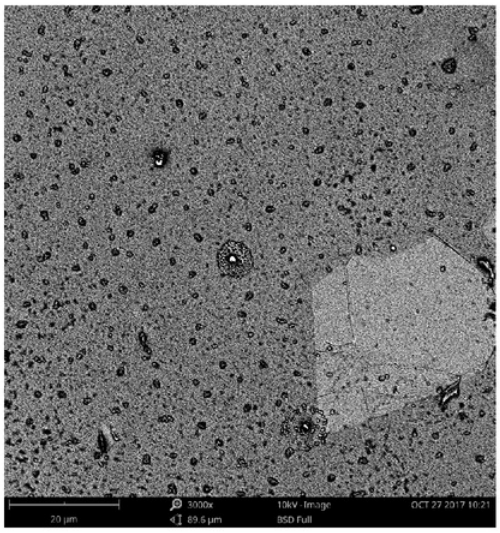

Figure 4.23: BSD image of Zn-0.8Sr at 20µm

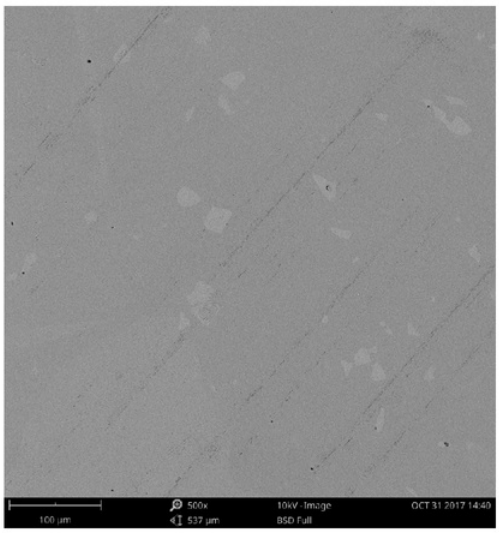

Figure 4.24: Clearer SEM image of Zn-0.8Sr

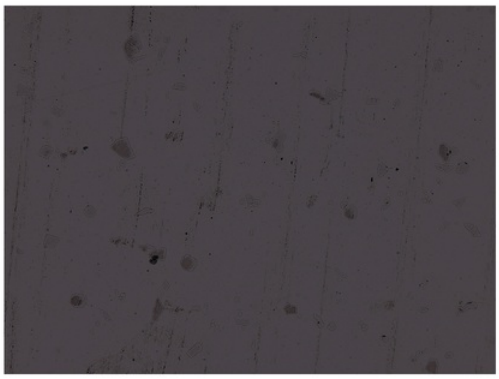

Figure 4.25: Optical image of Zn-0.8Sr

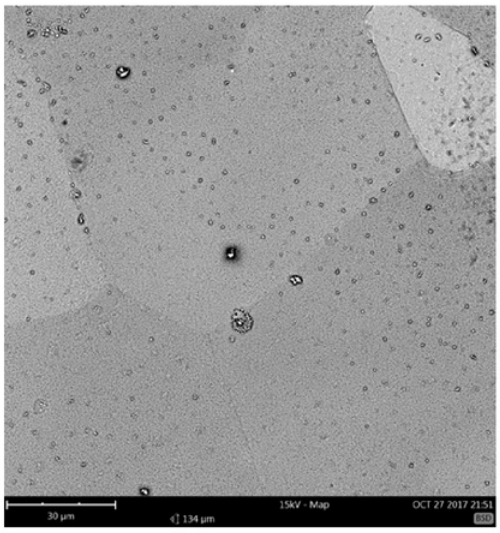

Figure 4.26: Combined mapping of Zn-0.8Sr

could possibly bring the value to exact. To determine the intermetallic phase at the point (4.28), it is assume that the intermetallic phase are made up $ZnSr_{13}$ as it is the closest to Sr 0.8 wt.%. The ratio of the $ZnSr_{13}$ can be calculated as $\frac{1}{14} = 7at.\%$, this value is fairly similar to Sr 8.90 at.% (4.13), proving that the intermetallic phase consist of $ZnSr_{13}$.

Table 4.12: Mapping Data of Zn-0.8Sr

Element Number	Element Symbol	Element Name	Atomic Conc.	Weight Conc.
30	Zn	Zinc	98.94	98.59
38	Sr	Strontium	1.06	1.41

Table 4.13: Point Data of Zn-0.8Sr

Element Number	Element Symbol	Element Name	Atomic Conc.	Weight Conc.
30	Zn	Zinc	91.10	88.42
38	Sr	Strontium	8.90	11.58

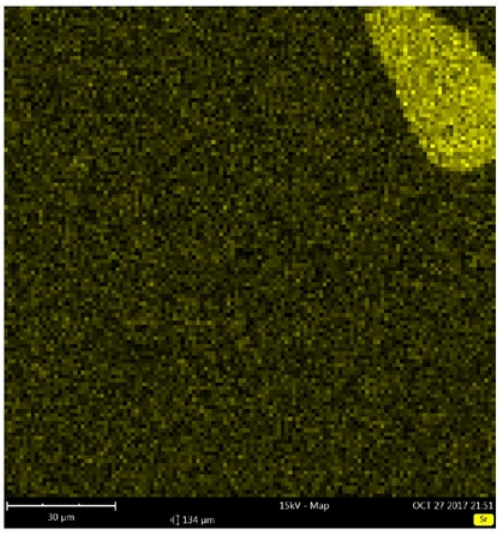

Figure 4.27: Strontium concentration

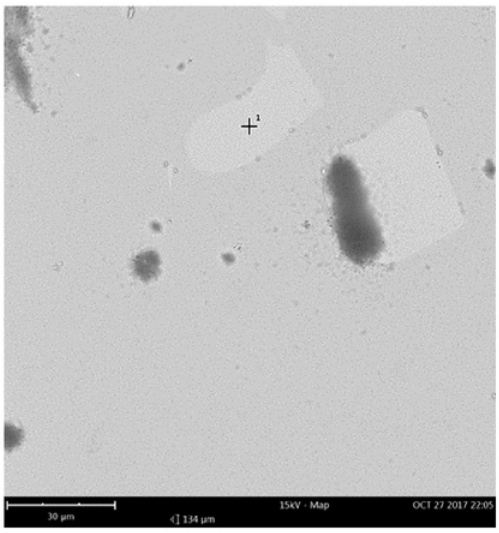

Figure 4.28: Point of Zn-0.8Sr

Chapter 5

Discussions

Biodegradable metals are constantly being further researched to improve its properties that allow it to be apply in medical implants. As mentioned pure Zn has been recently introduced as new candidate for biodegradable material. However with the mechanical properties of Zn being low, studies such as this thesis are looking into what other elements can be utilised to enhance the properties of Zn. The three elements (Mg, Ca and Sr) were considered as alloying element for Zn due to them being non-toxic to the human body and the elements found are available in the human system. Judging by the results it shows us that the Zn-alloys have enhanced the properties of pure Zn. The thesis was only able to look into the hardness values, if time weren't a constraint the thesis would of included more detailed mechanical properties, such as tensile testing. Unfortunately with the induction furnace not functioning, different wt.% compositions weren't available to be compared with. In summary, comparing the three Zn-alloys, Zn-Mg alloy had a better mechanical property than the other alloys due to the eutectic structure being a mixture of Zn and intermetallic phase.

Chapter 6

Conclusions

Based on the results obtained during this thesis, has been a successful with characterisation and with more time put into further studying Zn-Mg, the alloy can soon be applied into the medical fields, benefiting both patients and doctors . Characterisation of the Zn-alloys were made possible with the equipment supplied by the university. Problem were overcome during the process of making the alloy with the furnace not functioning, but with the guidance of Dr Wei Xu progress had resumed.

Chapter 7

Future Work

7.1 Characterisations

This thesis details the characterisations of the zinc alloys but only the microstructures and one mechanical properties have been analyse. Therefore requires further research into the mechanical properties of zinc alloy to further understand the alloy. The key properties to be analysed is the strength, corrosion resistance and reactivity, as the use of the zinc alloy will be applied into medical implants, such as cardiovascular stents, bolts and plates.

7.2 3d-printing

The main focus of this thesis is to characterise zinc alloy, in 7.1 it mentions that that there are further research to be analyse. The aim 'Can a novel zinc-magnesium alloy be successfully characterised, and successfully 3-d printed?', the second part suggest that it should be successfully 3-d printed, therefore the alloy is to have a low melting temperature which is capable of being printed from a Fused deposition modelling (FDM) printer. This research leads onto Marlon Leong's thesis 'Mechanical Properties of 3D Printed Parts and Discovering Zinc Fused deposition modelling'.

Chapter 8

Abbreviations

Zn	Zinc
Mg	Magnesium
Ca	Calcium
Fe	Iron
Sr	Strontium
SEM	Scanning Electron Microscope
XRD	X-ray Diffractometer
SiC	Silicon Carbide
dia	Diameter
FDM	Fused deposition modelling
BSD	Backscatter Diffraction
SED	Secondary Electrons
EDS	Energy Dispersive X-ray Spectroscopy

Appendix A

Method for grinding and polishing Zn alloys

Grinding

Step	PG	FG 1	FG 2	FG 3
Surface	SiC Foil #320	SiC Foil #500	SiC Foil #1200	SiC Foil #4000
Abrasive Type				
Lubricant Type	Water	Water	Water	Water
Speed (rpm)	300	300	300	300
Force (N) / Specimen	15	15	15	15
Holder direction	>>	>>	>>	>>
Time (min)	01:00	01:00	01:00	01:00

Polishing

Step	P 1	P 2	OP
Surface	MD-Mol	MD-Nap	MD-Chem
Abrasive Type	DiaPro Mol R 3 µm	DiaPro Nap R 1 µm	OP-S, 0.04 µm
Lubricant Type			
Speed (rpm)	150	150	150
Force (N) / Specimen	30	20	10
Holder direction	>>	>>	><
Time (min)	03:00	02:00	02:00

Figure A.1: Method from Sturers [12]

Appendix B

Project Plan and Attendance Form

B.1 Overview

This section will consist of the project plan that will be followed during the semester. This section will also contain the consultation meeting attendance form, required by this unit course.

B.2 Project Plan

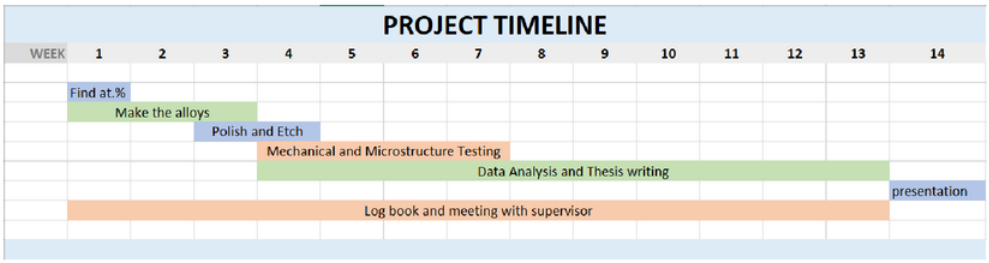

Figure B.1

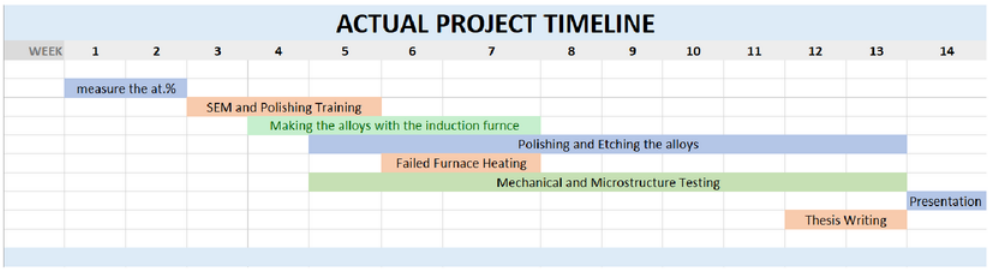

Figure B.2: Actual Project Plan

B.3 Attendance Form

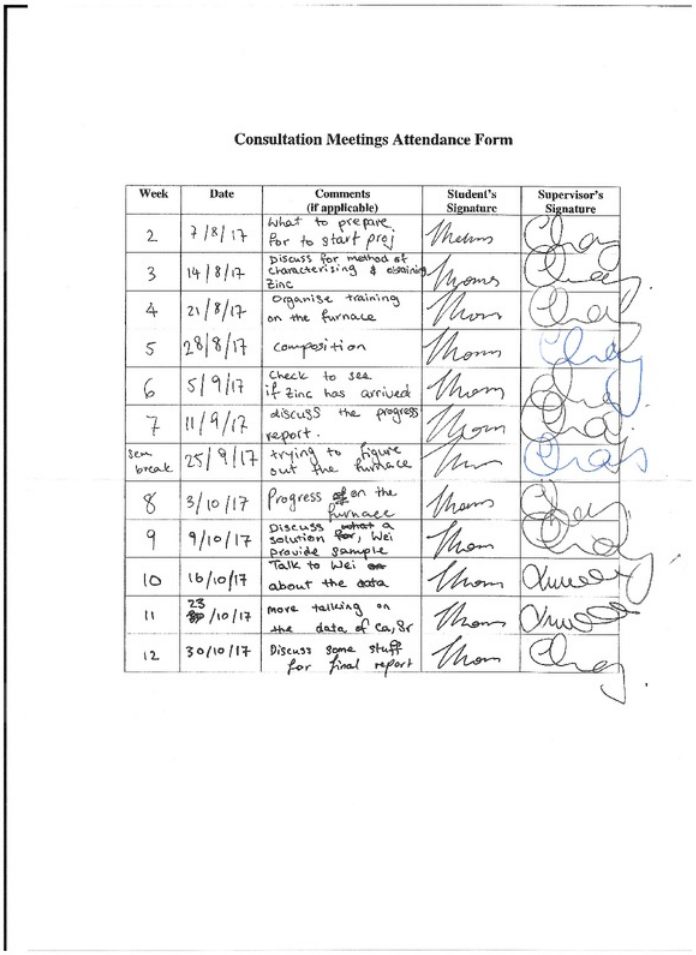

Consultation Meetings Attendance Form

Week	Date	Comments (If applicable)	Student's Signature	Supervisor's Signature
2	7/8/17	What to prepare for to start proj		
3	14/8/17	Discuss for method of characterising & obtaining Zinc		
4	21/8/17	Organise training on the furnace		
5	28/8/17	composition		
6	5/9/17	Check to see if Zinc has arrived		
7	11/9/17	discuss the progress report.		
Sem break	25/9/17	trying to figure out the furnace		
8	3/10/17	Progress ~~of~~ on the furnace		
9	9/10/17	Discuss ~~what~~ a solution ~~for~~, Wei provide sample		
10	16/10/17	Talk to Wei ~~on~~ about the data		
11	23 ~~30~~/10/17	more talking on the data of Ca, Sr		
12	30/10/17	Discuss some stuff for final report		

Figure B.3: Attendance Form

References

[1] N. Manam, W. Harun, D. Shri, S. Ghani, T. Kurniawan, M. Ismail, and M. Ibrahim, "Study of corrosion in biocompatible metals for implants: A review," *Journal of Alloys and Compounds*, vol. 701, pp. 698–715, 2017.

[2] J. Ma, M. Thompson, N. Zhao, and D. Zhu, "Similarities and differences in coatings for magnesium-based stents and orthopaedic implants," *Journal of Orthopaedic Translation*, vol. 2, pp. 118–130, 2014.

[3] H. Gong, K. Wang, R. Strich, and J. G. Zhou, "In vitro biodegradation behavior, mechanical properties, and cytotoxicity of biodegradable Zn–Mg alloy," *Society For Biomaterials*, vol. 103B, pp. 1632–1640, 2015.

[4] H. F. Li, X. H. Xie, Y. F. Zheng, Y. Cong, F. Y. Zhou, K. J. Qiu, X. Wang, S. H. Chen, L. Huang, L. Tian, and L. Qin, "Development of biodegradable Zn-1X binary alloys with nutrient alloying elements Mg, Ca and Sr," *Scientific Reports*, 2015.

[5] D. Vojtech, J. Kubsek, J. erk, and P. Novk, "Mechanical and corrosion properties of newly developed biodegradable Zn-based alloys for bone fixation," *Acta Biomaterialia*, vol. 7, pp. 3515–3522, 2011.

[6] J. Kubsek, D. Vojtch, E.Jablonsk, I.Pospilov, J.Lipov, and T.Ruml, "Structure, mechanical characteristics and in vitro degradation, cytotoxicity, genotoxicity and mutagenicity of novel biodegradable Zn–Mg alloys," *Materials Science and Engineering C*, vol. 58, pp. 24–35, 2016.

[7] E. Willbold, K. Kalla, I. Bartsch, K. Bobe, M. Brauneis, S. Remennik, D. Shechtman, J. Nellesen, W. Tillmann, C. Vogt, and F. Witte, "Biocompatibility of rapidly solidified magnesium alloy RS66 as a temporary biodegradable metal", journal="Acta Biomaterialia," vol. 9, pp. 8509–8517, Feb 2013.

[8] X. Gu, X. Xie, N. Li, Y. Zheng, and L. Qin, "In vitro and in vivo studies on a Mg–Sr binary alloy system developed as a new kind of biodegradable metal," *Acta Biomaterialia*, vol. 8, no. 6, pp. 2360 – 2374, 2012. [Online]. Available: http://www.sciencedirect.com/science/article/pii/S1742706112000827

[9] B. Predel, *Mg-Zn (magnesium-zinc)*. Berlin, Heidelberg: Springer Berlin Heidelberg, 1997, pp. 1–4. [Online]. Available: https://doi.org/10.1007/10522884_2026

[10] H. Okamoto, "Ca-Zn (calcium-zinc)," *Journal of Phase Equilibria and Diffusion*, vol. 34, no. 2, pp. 171–171, Apr 2013. [Online]. Available: https://doi.org/10.1007/s11669-012-0180-3

[11] ——, "Sr-Zn (strontium-zinc)," *Journal of Phase Equilibria and Diffusion*, vol. 29, no. 1, pp. 127–127, Feb 2008. [Online]. Available: https://doi.org/10.1007/s11669-007-9235-2

[12] Struers. (2017) Zinc and Zn Alloys (Very soft, DiaPro). [Online]. Available: "https://e-shop.struers.com/DK/EN/methods/Non-Ferrous_Metals/Zinc_and_Zn_Alloys/Zinc_and_Zn_Alloys_(Very_soft_DiaPro)(1789).aspx"

[13] H. S. Brar, J. Wong, and M. V. Manuel, "Investigation of the mechanical and degradation properties of Mg–Sr and Mg–Zn–Sr alloys for use as potential biodegradable implant materials," *Journal of the Mechanical Behavior of Biomedical Materials*, vol. 7, no. Supplement C, pp. 87 – 95, 2012, 7th TMS Symposium on Biological Materials Science. [Online]. Available: http://www.sciencedirect.com/science/article/pii/S1751616111002189

[14] A. F. Cipriano, A. Sallee, R.-G. Guan, Z.-Y. Zhao, M. Tayoba, J. Sanchez, and H. Liu, "Investigation of magnesium–zinc–calcium alloys and bone marrow derived mesenchymal stem cell response in direct culture," *Acta Biomaterialia*, vol. 12, no. Supplement C, pp. 298 – 321, 2015. [Online]. Available: http://www.sciencedirect.com/science/article/pii/S1742706114004607

[15] R. guo Guan, A. F. Cipriano, Z. yong Zhao, J. Lock, D. Tie, T. Zhao, T. Cui, and H. Liu, "Development and evaluation of a magnesium–zinc–strontium alloy for biomedical applications alloy processing, microstructure, mechanical properties, and biodegradation," *Materials Science and Engineering: C*, vol. 33, no. 7, pp. 3661 – 3669, 2013. [Online]. Available: http://www.sciencedirect.com/science/article/pii/S092849311300283X

[16] B. Homayun and A. Afshar, "Microstructure, mechanical properties, corrosion behavior and cytotoxicity of Mg–Zn–Al–Ca alloys as biodegradable materials," *Journal of Alloys and Compounds*, vol. 607, no. Supplement C, pp. 1 – 10, 2014. [Online]. Available: http://www.sciencedirect.com/science/article/pii/S092583881400872X

[17] Y. Zheng, X. Gu, and F. Witte, "Biodegradable metals," *Materials Science and Engineering: R: Reports*, vol. 77, no. Supplement C, pp. 1 – 34, 2014. [Online]. Available: http://www.sciencedirect.com/science/article/pii/S0927796X14000023

[18] F. Witte, "Reprint of: The history of biodegradable magnesium implants: A review," *Acta Biomaterialia*, vol. 23, no. Supplement, pp. S28 – S40, 2015. [Online]. Available: http://www.sciencedirect.com/science/article/pii/S174270611500313X